California State University, Fresno

Lyles College of Engineering

Electrical and Computer Engineering Department

Technical Report

Project Title: Multi-source Energy Harvesting for Wireless Sensor Networks

Course Title: ECE186B - Senior Design II

Date Submitted: May 11, 2020

Prepared by:

Alwin Villamor, Lee Lor, Lawrence Brieno III

Faculty Advisors:

Dr. Woonki Na, Dr. Nan Wang

INSTRUCTOR SECTION

Comments:____

____

____

____

Final Grade: Team member 1: ______________

Team member 2: ______________

Team member 3: ______________

TABLE OF CONTENTS

1. Statement of Objectives

Wireless sensor networks have many applications. For instance, a cause of concern that the wireless sensor network could solve is forest fires in remote regions. This issue could be mitigated by placing sensor motes in various locations around a region and then observing and recording the surroundings every specified interval. These recordings would then be uploaded to a local storage or cloud. Should there be any anomaly to the surroundings, the sensor mote would notify other surrounding sensor motes and a relay of communications between nearby sensor motes will take place. Ultimately, these sensor motes would determine the location of the anomaly and update the information to a local storage or cloud. Such information can be used by firefighters, or professionals alike, to quickly determine the location of an emergency and prevent it before the issue becomes too precarious. Many natural disaster relief systems could also utilize wireless sensor networking to achieve a similar effect to ensure a quicker response time by rescue teams. But while there are many possible usages for them but one negative aspect that is limiting these applications is the power inefficiency. This will be the main focus in this project. A hybrid energy harvesting system be designed and implemented to tackle this particular issue.

The primary objective of this project is to design and implement an efficient multi-source energy harvester system that will be used to efficiently power a sensor node or mote. A network of sensor nodes will be designed to ensure that the energy harvester is functioning correctly and that the sensor node is operational; these nodes will wirelessly communicate with one another. There were two original components of the project which consist of both electrical and computer engineering knowledge. These goals have shifted after getting feedback from our advisor, Dr. Wang, and the primary focus is just on the hybrid energy harvesting aspect. There are many energy sources that can be used to power the sensor node - in this project, the primary focus will be on wind and solar power. These energy sources will be incorporated and managed by circuit design to effectively output power for the wireless sensor network mote. With a multi-source energy harvesting system, the pathways providing power will be critical, as such, many discretations were made during the design and simulation process.

2. Technical Plan

2.1:Introduction

Energy harvesting is the process of capturing energy from ambient sources such as solar power, thermal energy, wind energy, etc (aka ambient energy) and storing them to use for small wireless autonomous devices - such as wireless sensor networks (WSN). In this project, two ambient sources will be used to power the WSN - namely solar and wind energy. The energy harvesting device will convert the ambient source into electrical energy. This will allow the WSN to be self-sufficient and last longer which will allow it to be more useful for deployment in harsh or isolated environments.

The following are possible energy sources that could be harvested to power the sensor mote. The sensor mote will be the base point of connecting the sensor nodes that will communicate wirelessly.

Solar Power:

- Solar power is generated by light sources; these sources can be indoors or outdoors. We will primarily focus on outdoor light sources. Solar power can be generated by using solar panels. Solar panels work by gathering photons from the sun and dispersing them in silicon-composite materials.
- A virtual solar panel is required for testing to ensure that it outputs the correct values. This can be done by representing it with an equivalent circuit. The equivalent circuit for a solar panel is given in figure 2.3. This presentation will be used to simulate the solar panel to ensure that the implementation of the solar panel outputs the necessary and correct values for the load.

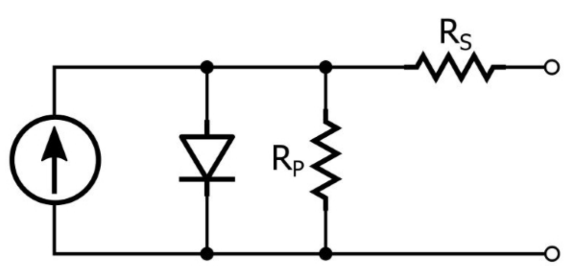

Figure 2.1.1: Solar panel equivalent circuit [2].

Wind power:

- Wind power can be generated through using a small wind turbine. The propellers in the turbine are connected to a rotor that is connected to a shaft. This shaft is connected to a generator such that when the shaft spins, electrical energy is generated [1].
- Similar to the solar panel, the wind turbine can be represented virtually. The equivalent circuit of a wind turbine is given in figure 2.4. This circuit will be used to simulate the wind turbine to achieve the desired effect.

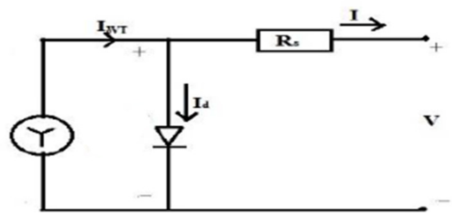

Figure 2.1.2: Wind turbine equivalent circuit [4].

Thermal power:

- Thermal electricity is achieved when heat flux is converted to electricity. This can be done through having a small thermoelectric generator. This generator works by taking the thermal gradient of two different conductive surfaces.

2.2 MPPT

In order to efficiently harvest energy from the two devices, that will be utilized in this project, a maximum power point tracking (MPPT) algorithm must be implemented. This will output the duty cycle which the converters will use to get the maximum power to charge the battery. In the past, we have investigated in multiple MPPT techniques, and we have found three promising algorithms: Perturb and Observe (P&O) also known as the hill climbing algorithm (solar), Tip Speed Ratio (TSR), and Incremental Conductance (INC). These are part of the direct MPPT which has a faster response in comparison to the indirect MPPT. To visualize their mean duty, figure 2.2.1 shows the power curve and current-voltage source. In order to get the maximum power out of the harvesting devices, the current and voltage must be in the knee on the current-voltage curve and the top of the power curve. This will ensure the efficiency of our system.

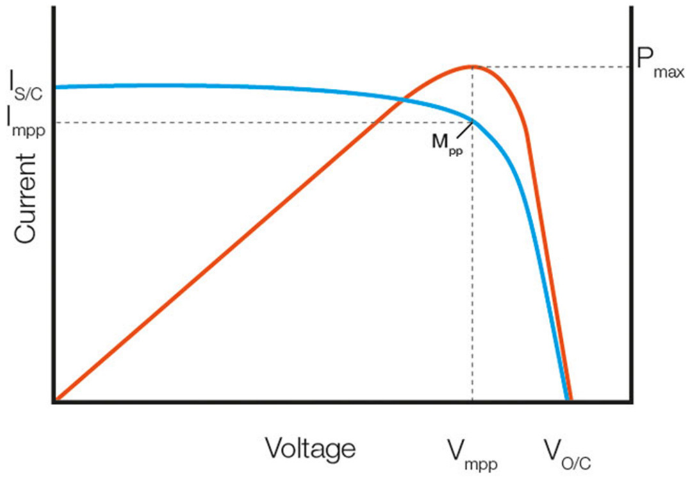

Figure 2.2.1: PV module outlining the MPP

https://www.seaward-groupusa.com/userfiles/curve-tracing.php

2.2.1 Perturb and Observe (P&O)

This technique was originally going to be used for the solar device. To achieve the maximum power point (MPP), the algorithm operates in the following fashion. Should there be a voltage increase that results in an increase in power, then perturbation is needed to the right of the curve. Conversely, if an increase in voltage leads to a decrease in power then perturbation is needed to the left. This technique takes advantage of the nature of the PV curve which shows that an increase of power is to the left of the MPP and a decrease is to the right of the MPP. The downside with this technique, however, is that the operating power is never steady in the MPP and only hovers around it. There is also a need to mention that it struggles in rapidly changing weather conditions which is an important design factor. Thus if we were to choose this design, location placement will matter.

2.2.2 Tip Speed Ratio (TSR)

This technique was originally going to be utilized for the wind device. To achieve the MPP, the algorithm works in the following fashion. Kinetic energy (which is the wind in this case) is transformed into mechanical energy to run a generator which will then generate electrical energy. This relationship is provided by the equation 2.2.1.

Equation 2.2.1:

$$□ = (1/2)□□^{2}□^{3}□□(□,□)$$

In the above equation. the □is the air density (kg/m^3), R is the turbine rotors (m), V is the wind speed (m/s), and C_p(□,□) is the coefficient of performance [6]. The most important part of this equation is the turbine power coefficient (C_p). The   is the tip speed ratio where the MPPT is derived. The tip speed ratio requires another formula. Equation 2.2.2 shows how the TSR can be mathematically obtained, where ω is the mechanical angular velocity. If the TSR maintained constantly at its optimal value, then there is certainty in obtaining the MPP [6]. Unfortunately, this method requires a consistent and accurate measurement of wind speed. This requires more hardware which will potentially make our hybrid system bigger which is going against our original intentions - to make it compact and as small as possible.

Equation 2.2.2:

$$= (\quad)/$$

2.2.3 Incremental Conductance (INC)

This last technique is what we are going to be using for both the solar and wind. For solar, it takes the P&O method and makes it better by fixing the drawback. This technique checks the instantaneous conductance (I/V) and the incremental conductance (dI/dV). When these two are the same then the voltage is the MPP. The observation of the MPPT is in regards to the change in power over the change in voltage. If this change is 0, this is where the maximum power will be harvested. The equation shown in 2.2.3 shows the relationship of the description given above to the MPP [7].

Equation 2.2.3:

$$\frac{\square\square}{\square\square} = -\frac{\square}{\square} V_p = V_{MPP}$$

$$\frac{\square\square}{\square\square} > -\frac{\square}{\square} V_p < V_{MPP}$$

$$\frac{\square\square}{\square\square} < -\frac{\square}{\square} V_p > V_{MPP}$$

As for the wind, it removes the extra hardware needed to measure the wind speed. This technique utilizes the same equation 2.2.1 described above, but rather than maximizing the mechanical power using the TSR, this technique uses the Pitch angle (β). The pitch angle is the angle between the direction of wind and the direction perpendicular to the plane of the blade [7].

2.3 Power Efficiency Convertor

One constraint that many WSNs face is power consumption and in this project, we will face this by implementing a hybrid power source which we hope will enable the WSN to operate for longer amounts of time in the field with little to no human interactions.

After many considerations, two energy sources were chosen due to their availability and efficiency. The two tentative energy sources that will be focused on in this project are wind and solar. In order for the sensor mote design to operate, these energy sources must be efficiently converted, and then stored. For reference, the average power used by a wireless sensor node is given by equation 2.3.1, where D is the duty cycle and P is the power [3]. This equation will be referenced to ensure our conversion circuits are efficient.

Equation 2.3.1:

□□□□ = □ ∗ □□□□□□□ + (1 − □) ∗ □□□□□□

Our first objective will be to implement the energy source harvester and converter. Depending on the energy source, the implementation will vary. Ultimately, we will assimilate these energy sources and convert them to electrical power; ideally these energy sources will power the same battery. This will be done through conversion circuits. The bidirectional buck-boost converter will be used to regulate the charge voltage and current supplied to the lithium ion battery; figure 2.3.1 shows the general design of the two-switch buck-boost converter that can be used to achieve this purpose. Q1 and Q2 are switches that will enable buck or boost mode. At a certain duty cycle, Q1 will be enabled and the converter circuit will be in buck mode; the same applies when Q2 is enabled at a specified duty cycle. The duty cycle for the buck and boost converter is given below and will be used to configure this circuit.

Equation 2.3.2:

□ □□□□ = □□ / □□

1 / (1 − □ □□□□□) = □□ / □□

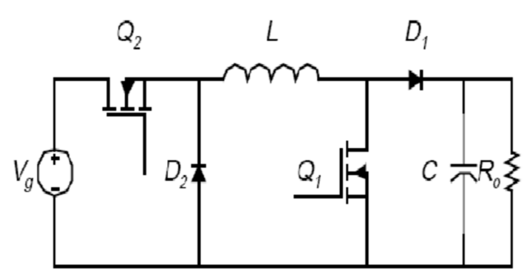

Figure 2.3.1: Two-switch buck-boost converter circuit.

https://www.researchgate.net/figure/Two-switches-Buck-Boost-converter_fig1_268407684

This two-switch buck-buck converter circuit was considered because of its efficiency and simplicity. The configuration of this converter circuit allows so that one switch at a time operates and only one mode is configured as opposed to having two modes simultaneously on and operating. This buck-boost converter will allow so that the voltage and current supplied to the battery is within ±1 % error. This will be done by modifying the duty cycle of the buck and boost converters; doing this will ensure that the ripple of the voltage does not exceed a specified value (in this case within 1% error). This modification will be done through the MPPT where the suitable voltage and current will be selected. A feedback control loop will also be implemented to further enhance this. Simulations of the two-switch buck-boost converters will be done with PSIM and multisim. Simulations will account for low voltage sources to ensure that the design operates in worse-case scenarios.

After electrical power is generated and converted, it will be stored in the battery to power the sensor node and the micro-controllers that are used - which is about 3.3 v. There will be a power management system to ensure that the power is efficiently used and that the overall system is operating within its intended power limits; this can be achieved through an algorithm. If the power is controlled correctly, then the device being powered should operate efficiently. Figure 2.3.2 shows the general method of this design.

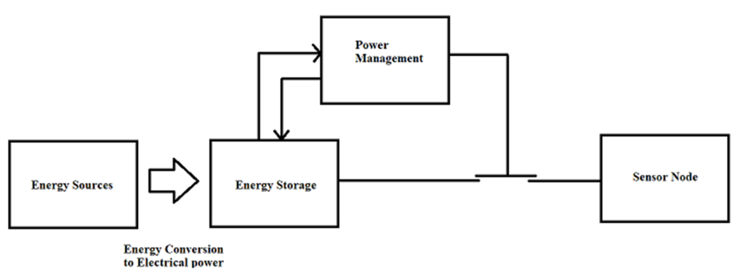

Figure 2.3.2: General method of designing the energy harvesting system.

After several issues with designing the two-switch buck boost converter, we came up with three designs for hybrid energy utilization. The first design incorporated the use of op-amps. This design is shown in figure 2.3.3. In this design, a summing amplifier is used to add the voltages from the two hybrid sources. The summed voltage from these two sources will then be bucked or boosted to the desired voltage for the battery or load. This design is desirable because both sources will always be utilized and no source is left being used thereby increasing efficiency and max power output. The problem with this design is that we require voltage supplies for the power rails of the op-amp since the summing amplifier can only output voltages between the positive and negative power rails. Hence, we would need rather high voltages for the power rails of the op-amp if the sum of the two sources are high; this is most likely the case since the solar panel will provide a minimum of 4 v on a cloudy day. Thus we would require rather high power rails for the summing op-amp to ensure that summed voltage is outputted correctly. Thus, we had to defer to another design.

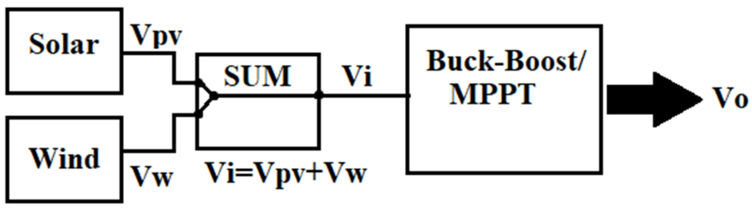

Figure 2.3.3: Design with summing amplifier for , hybrid energy harvesting.

The second design that was put into place was the utilization of a comparator switch as a node after the solar and wind harvester. This design is shown in figure 2.3.4. In this design, the switch will choose between either the solar or wind source; the switch would ideally be a mosfet where the gate will be controlled to close or open the switch. A voltage sensor was to be used to determine which voltage source was producing more voltage. The voltage source with the greater voltage would then be selected through the microcontroller. This voltage will be bucked or boosted with the buck-boost converter. The mppt will regulate the change so that it remains a constant 4.2 v for our usage. However, this design was inefficient because it failed to take into account the other unused source. For more efficient practices, we would want to use both sources. As such, design three combined both of design one and two to create an better and overall efficient source harvester system.

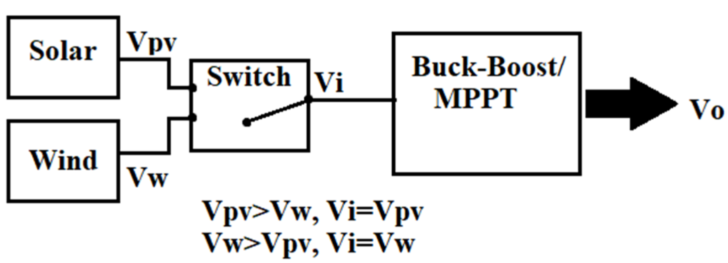

Figure 2.3.3: Design with comparator switch for hybrid energy harvesting.

The third design is shown in figure 2.3.4. In this design, both solar and wind sources are being utilized. Both sources will be bucked or boosted to the correct output voltage of 4.2. The output terminals of both sources will then be connected in parallel as shown in the figure. This is to ensure that both sources are being used, and should one fail - one will always be working to power the load. The load, in this case, is the sensor mote. A capacitor will be placed before it to store the energy that will be coming out of the buck and boost converter. The battery, meanwhile, will need a bidirectional buck-boost converter. This configuration is set so that the terminals from the solar and wind converters can charge the battery. The battery can then discharge to the terminals via the bidirectional buck-boost converter which thereby powers the load should there be no power coming from the solar and wind converters. This design compensates for a scenario where both sources are not outputting enough power to supply the sensor mote. However, this scenario required some trade offs as well. Firstly, if one of the sources is not outputting enough power, then the voltage at the terminals will not agree - which will affect the stability of the output. This instability will cause issues to the load and the battery. In order to avoid this issue, we must turn off the source that is not providing enough energy. This can be implemented by using the microcontroller to turn off the mosfet switches of the buck or boost converter. Doing so will ensure that the voltages from the buck and boost converters don't fight one another and cause instability. We also might incorporate mosfet switches in between the terminals as another precautionary measure to ensure this scenario does not occur. Once implemented correctly, the design should be able to efficiently manage and power a sensor mote for a relatively lengthy amount of time.

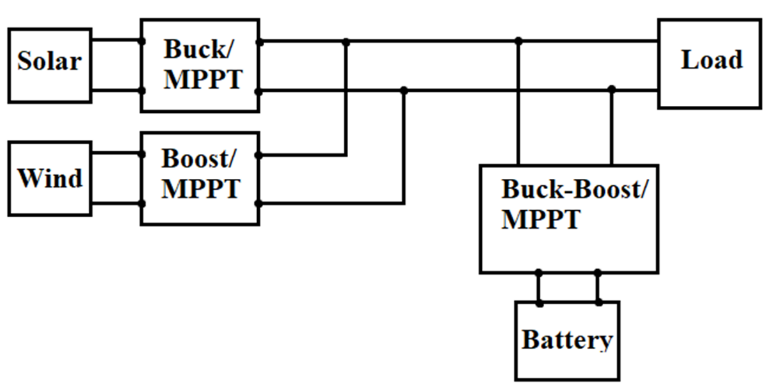

Figure 2.3.4: Final design for hybrid energy harvesting.

2.4 DC Converters Design

The desired output for the DC converters is to be 4.2 volts and 0.3 amps. In order to obtain these values, the converters need to have specific capacitor and inductor values. Both the buck and boost converters have to stabilize the output values within a 1% error. These considerations were made during the designing process of the buck and boost converters, because the li-ion battery being used is sensitive to current spikes and could lead to damage or worse. First, the design for the buck converter will be taken into consideration. In order to accomplish the specifications, the equations seen in Equation 2.4.1, were used to calculate the capacitor and inductor values so that the buck converter will output our desired values.

Equation 2.4.1:

$$L_{min} = \frac{(V_i - V_o)D}{f_s \cdot \Delta i_L}$$

$$C_{min} = \frac{1 - D}{8 L_{min} \cdot (\Delta V_o / V_o) \cdot f_s^{2}}$$

In equation 2.4.1, only the minimum inductor and capacitor values are given; in order to ensure continuous conduction mode (CCM), these values will need to be multiplied by a factor of 3 as a precautionary measure. Both equations will require the same duty cycle (D) and switch frequency (f_s); it will also require knowledge of input voltage (Vi), current ripple of inductor (ΔiL), and output voltage (Vo). Recall that the duty cycle of a buck converter is output voltage over the input voltage. Equation 2.3.2 demonstrates this. Thus if we want a desired voltage Vo, we can determine and set a select duty cycle if we are limited by the input voltage - which in this case is a 6v solar panel. However, solar panels produce variable DC voltages and this changing input will cause instability to the output. To compensate for this, we factored in the worst-case scenario for our converter so that our capacitor and inductor values can withstand extreme levels of voltage. Since the buck converter steps down voltage, in the worst case, it will need to buck the maximum voltage from the source. The maximum voltage that can be produced from the solar panel will be around 12 v. Hence, we will calculate our values based on these assumptions. The selected switch frequency was 200 kHz. This range was selected to ensure that our components remain cheap and small while also maintaining stable output - with the drawback being only noise. The current ripple of the inductor can also be assumed based on our desired current ripple of our output since the current of both the inductors and output will be equal to each other after a certain amount of time has passed. The output voltage ripple is restricted by the ratings of our battery. With these known variables, we can effectively calculate our values for the buck and boost converters. These results are shown in our simulation designs.

The next converter that was designed was the boost converter for the wind source. This converter was selected to step up the voltages of the wind harvester because wind relative to solar, will always be lower in these regions. And since the boost converter steps down voltage, in the worst case, it will need to boost the minimum voltage from the source. The minimum voltage that can be produced from the wind harvester will be around 1 v. Hence, we will calculate our values based on these assumptions and by using equation 2.4.2. The selected switch frequency is the same value as used in the last calculation - 200 kHz. The variables all still have the same definitions: input voltage (Vi), duty cycle (D0), current ripple of inductor (ΔiL), switch frequency ($□_{□}$), output voltage ripple (ΔVo), and output voltage (Vo). These known variables can then be used to calculate our component values. The results are shown in the simulation designs.

Equation 2.4.2:

$$□□□□ = \frac{□□ \cdot □}{□_{□} \cdot □□_{□}}$$

$$□□□□ = \frac{□}{□□(□□_{□}/□□) \cdot □_{□}}$$

The final converter that was designed was the bidirectional buck-boost converter. The task of this converter was to charge and discharge the lithium-ion battery. This means that we have to buck the 4.2 volts coming from the output terminals of the buck and boost converters of the solar and wind harvesters to the battery. And should there not be enough power output at the terminals of the converters, the bidirectional converter will discharge the battery and boost its nominal output voltage to 4.2 to supply the load. As such, this converter will manage the power of our entire system. To design this converter, we have to account for buck-mode and boost-mode. The equations used to calculate for the inductance for buck-mode and boost-mode are shown in equation 2.4.3. In these equations, D1 represents the duty cycle in buck-mode and D2 represents the duty cycle in boost-mode. The voltages Vb and Vo represent the voltage of the battery and the voltage at the output terminals of the solar and wind converters respectively. The voltage and current ripples will remain within the 1% error; voltage ripple and current ripple are represented as ΔVo and ΔiL respectively. The frequency switch of this converter will remain the same as the one used in previous designs. The results are shown in the simulation designs.

Equation 2.4.3:

$$\square 1 = \frac{\square\square}{\square\square}, \quad D2 = \frac{\square\square - \square\square}{\square\square}$$

$$\square\square\square\square = \frac{\square\square \cdot \square 1 \cdot (1 - \square 1)}{\square_{\square} \cdot \square\square_{\square}}, \square\square\square\square = \frac{\square\square \cdot \square 2}{\square_{\square} \cdot \square\square_{\square}}$$

$$\square = \square\square \frac{\Delta \square}{\square\square_{\square}}$$

2.5 Power Storage

In general, energy is stored in capacitors, supercapacitors, or batteries. The original goal was to utilize a lithium ion battery and supercapacitor. There are reasons for this. The battery was chosen as energy storage because batteries leak energy which is useful in providing a steady flow of energy. The supercapacitor was considered because of its virtually unlimited charge-discharge cycles that can theoretically operate forever to enable a maintenance-free operation in WSN. However, after many considerations our group has decided on utilizing only one energy storage unit. We have decided on using a lithium-ion battery to power the sensor mote. The battery required for this operation will output 3.7 v and will require a boost dc/dc converter to step up the voltages to the desired voltage of 4.2 v for the sensor load. This function is achieved by the bi-direcitonal buck-boost converter. A design for the bi-directional buck-boost converter is shown below.

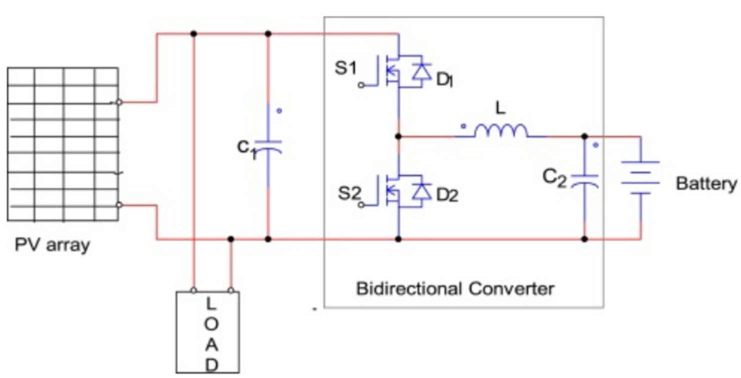

Figure 2.5.1: Bidirectional buck-boost converter for charge and discharge.

2.5.1 Lithium-ion Battery:

The lithium-ion battery will provide additional power to the sensor motes if the wind turbines and solar panels are offline. In times of no sun or wind, the lithium-ion battery will serve as a backup power source. However, one of the goals of this project is to design an efficient pathway of managing the power source flow. The lithium-ion battery must also have the right charging scheme, because lithium-ion batteries are sensitive to voltage and current spikes as well as temperature. The appropriate charging scheme, for the lithium-ion batteries, will be the constant-current constant-voltage (CCCV) charging scheme[5]. The constant-current constant-voltage charging scheme is displayed in Figure 2.5.2: CCCV with three stages, which illustrates a charging graph of the three main stages. These three main stages, for the CCCV scheme, are the trickle phase, constant-current phase, and constant voltage phase [5]. The first stage of charging is the trickle stage and serves a very important role for this scheme. The trickle stage is implemented to check and verify the conditions of the battery, such as testing if the battery is damaged or if it is properly working [5]. As seen in Figure 2.5.2, the trickle phase is only carried out for a short amount of time compared to the other two phases. This pre-set time will end once the current of the battery spikes, and then the second phase will begin. The constant-current phase is started once the trickle phase determines the battery is healthy and functioning [5]. However, if the battery isn't responding then the process of the charge is terminated. The constant-current phase will continue until the voltage of the battery is set a constant value, which is also seen in Figure 2.5.2 [5]. Finally, the last stage is the constant-voltage phase. This stage will provide charge to the battery until the current of the battery has dropped to the trickle boundary, as seen in Figure 2.5.2. With this charging scheme, the circuitry will be used as seen in Figure 2.5.3: CCCV switching implementation circuit.

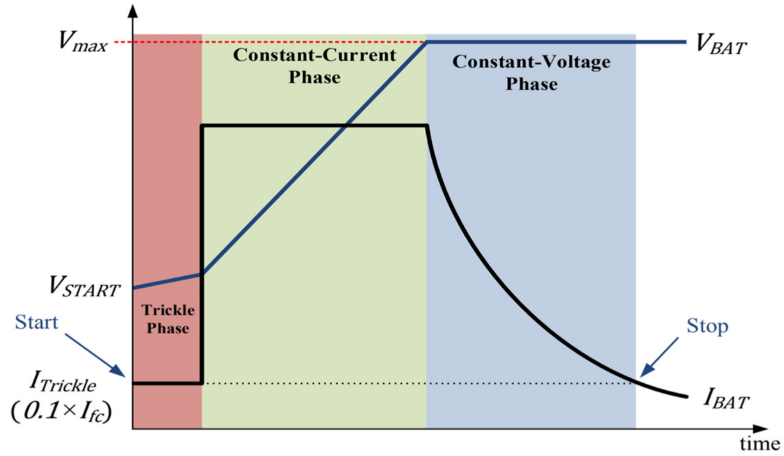

Figure 2.5.2: CCCV with three stages.

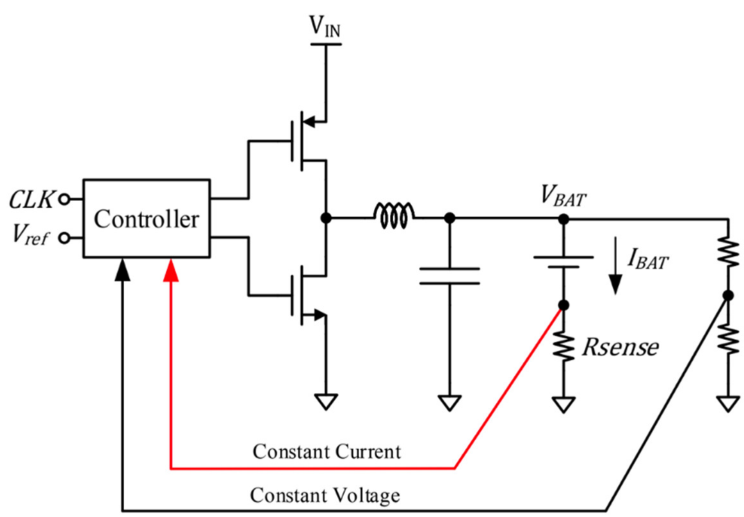

Figure 2.5.3: CCCV switching implementation circuit.

2.6 Microcontroller

There were two microcontrollers being studied for this project, STM32f103c6 and pic24fv16km102. The two had almost similar features needed for this project, which are ADC converter, used to sense the voltage and current, and PWM, to control the switches for the mosfets. This was the brain of the project housing the MPPT algorithm and the charging scheme for the lithium-ion battery.

The differences were that the pic24 was a 16 bit chip while the STM32 is a 32 bit chip meaning the STM32 is able to address more memory location than its counterpart. Most importantly, as for the required features the stm32 has up to 18 multiplex channels with an ADC converter a 12 bit of resolution and it has up to 4 general purpose timers which can be utilized to generate PWM output. Each of the timers has around 4 independent channels for generating the PWM. On the other hand the pic24 only has up to 19 channels with a 12/10 bit resolution and has up to 7 channels to output PWM.

In the beginning of this project, I decided to try to create my own microcontroller using the pic24 but due to a few challenges with some equipment not being accessible and little documentation on how to configure the registers, we decided to move ahead with using the STM32f103C8. Not only does this microcontroller have more output pins to utilize for our project but has more documentations.

For the MPPT and State-of-Charge (SoC) algorithm to work, the microcontroller takes inputs from the ADC channels connected to the battery and from the two ambient sources. My plan for the SoC was to enable the watchdog which has an upper and lower bound, which will correspond to the constant current and constant voltage explained above. If the channels connected to the battery exceeds the values that were set, it will enable an interrupt which will handle the charging mechanism. If the battery is in need of charging it will turn on the bidirectional buck-boost to start the process. Also, once the battery is almost at its maximum capacity it will send an interrupt which changes the current flow of the bidirectional converter, depending on the condition of the output of the ambient sources. If the two ambient sources are producing enough power, the battery will be on standby. Which means the ambient sources are going to be powering the sensor. If the sources are not providing sufficient power, the bidirectional converter will be turned on for the battery to discharge its power.

2.6.1 ADC

The STM32 microcontroller has several channels to utilize for Analog to Digital Converter. The ADC can be performed in single, continuous mode for a single channel, scan through all channels, externally triggered conversion, and a DMA request based conversions. This microcontroller uses the successive approximation register (SAR) principle. In which the conversion is performed in several steps. Each conversion step is equal to the number of bits in the ADC converter and is driven by the ADC clock. This clock can be configured to the optimal adc sampling rate. Most of this configuration will be handled by the STM32CubeMx, which allows programmers to easily configure necessary registers through a very simple GUI.

To convert the analog signal into digital format we are going to use the equation 2.6.1. The ADC value is divided by the resolution we choose and then multiplied by the reference voltage. For this MCU the reference voltage is 3.3 volts. Any voltage acquired by the sensor will only be sensed as 3.3V.

Equation 2.6.1

□□□□□ □ = (□□□ □□□□□ / □□□ □□□□□□□□□□) ∗ □□□□□□□□□ □

Another important aspect which needed to be confronted was how to read current using ADC modules. Fortunately, there are ICs out there which are made to convert current into voltage so microcontrollers can use its ADC, but unfortunately for us it would have taken until the end of the semester for those ICs to arrive. So, I decided to create my own converter using a shunt resistor. My current sensor includes a shunt resistor with 0.1 Ohms. This converters the current into voltage so the microcontroller can utilize the ADC module. The reason why a shunt resistor was used is because it has a very small value of resistance which in turn does not affect the circuit’s current significantly. Before the microcontroller takes in the voltage, the voltage out of the shunt resistor is first passed into a non-inverting amplifier with a decoupling capacitor on the output. The non-inverting amplifier is used to linearly scale a very low voltage drop across the shit with less than 1 volt to 0-3.3V to correspond with the 0-1A current. Lastly, the decoupling capacitor is used to minimize the loading effect caused by the device’s leakage current.

The voltage from the circuit is read using a voltage divider to make sure the voltage is in the range of the ADC (which is 0-3.3 V). The actual voltage is recalculated in software using Equation 2.6.2 rearranged with Vin being the value being determined. Also, to minimize the loading effect caused by the device's leakage current, the output voltage of the voltage divider is passed into a buffer amplifier with a decoupling capacitor. Scaling down an input signal to drive an ADC's full-scale range will significantly degrade the signal-to-noise ratio (SNR).

Equation 2.6.2

$$\square\square = \square\square\square\frac{\square 2}{\square 1 + \square 2}$$

2.6.2 PWM

The PWM module is an important part of this project to harvest the maximum output of the two energy sources. The PWM output pulses, which is controlled by the duty cycle. The duty cycle is the percentage of time a pulse is either on or off and this is going to be based on the equation provided above. To utilize the PWM output we will be using the general purpose timers the STM32 provides. Because there are 4 switches needed to control the Buck, Boost, and Buck/Boost, we will use 4 pins to generate the PWM.

3. Equipment, Budget, Work Completion, and Conclusion

3.1 Equipment and Budget:

The following proposed budget and equipment, for this project, is subject to change due to calculations, simulations, and future hardware discoveries that will optimize our design and make our cost efficient. In the moment, the hardware and the cost is proposed by the following:

1. Solar panels
2. Wind turbine generator
3. Sensor Mote(TelosB Sensor Mote)
4. Softwares (Matlab, PSIM, Contiki OS, MPLab X IDE & IPE, STM32CubeMX, Keil uVision)
5. Micro-Buck/Boost Converters
6. PIC16(L)F17779 / STM32F103C8 microcontroller

7. 1500mAh Li-Ion battery
8. TH (for prototyping) and SMD or DIP Passive Components
9. Solderless Breadboard

Table 3.1: Proposed Equipment Budget

Item	Cost
Sensor Mote	$100
Monocrystalline Solar Panel	$16
Small Wind Turbine - Two Units	$20
Micro Buck/Boost Converters	$3-8
Li-Ion Battery	$7
Microcontroller (3.3-5V)	$10
Schottky Diodes	$3
Miscellaneous	TBA
Perf Board	$10

The design approach of this project is a matter of various aspects, such as compactness, efficiency, and available hardware. In terms of compactness, our goal is to develop a Printed Circuit Board (PCB) design that will meet our calculations and simulations results. The PCB design is desired to be a surface-mount device (SMD), because it will reduce the board cost, materials handling cost, and significant manufacturing control process [8]. This will be the final approach to our design and the cost is not yet known.

3.2 Completed Work

The Buck DC/DC converter has been calculated and designed, with a voltage mode controller. The buck converter was successfully simulated in PSIM. The buck converter was calculated to be in Continuous Conduction Mode (CCM). The voltage mode controller was also designed in matlab with the selected crossover frequency. Appendix A shows the matlab code for the various calculation parameters. In Figure 3.2.1: The buck DC/DC converter, shows the circuit that was simulated in PSIM. When simulating the buck converter, the output voltage demonstrated to be stable. The regular buck converter is shown in figure 3.2.2. The boost DC/DC converter is shown in figure 3.2.3. The bidirectional buck-boost converter is shown in figure 3.2.4. This design is shown with the inductor and capacitor values that will be implemented. However, this is subject to change due to the incorporation of a microcontroller that will drive the PWM signals and also implement the control aspect of the converters.

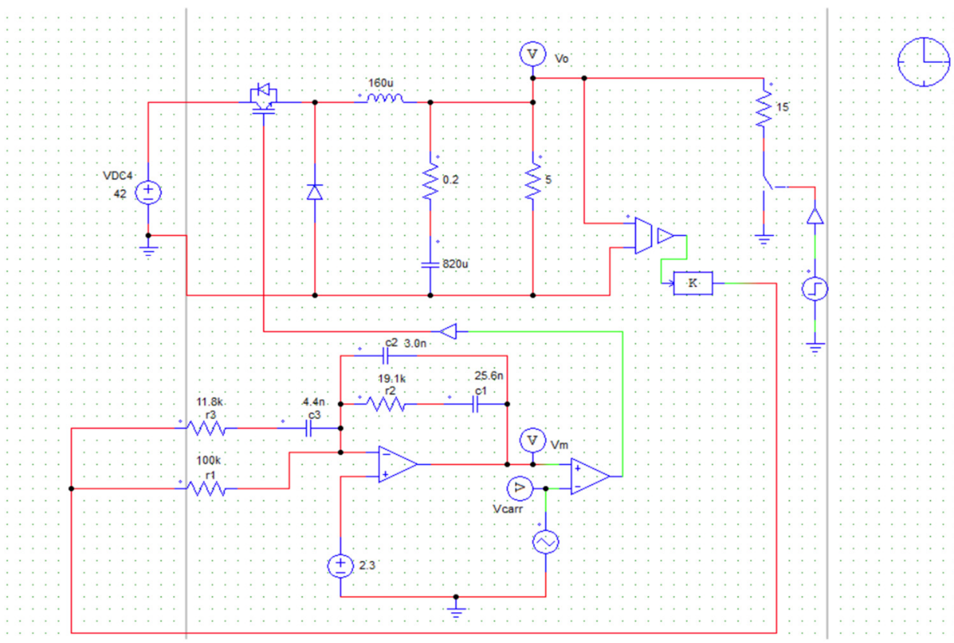

Figure 3.2.1: The buck DC/DC converter with compensator.

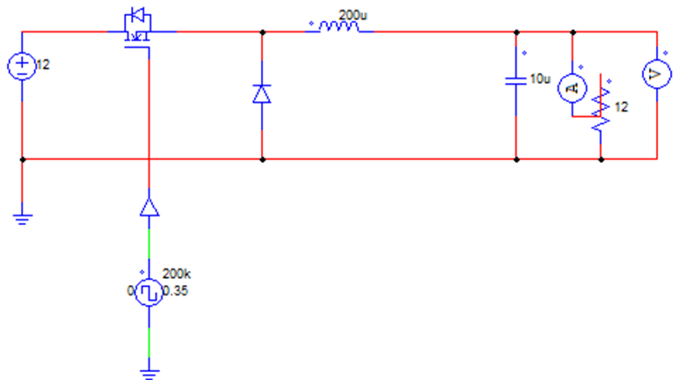

Figure 3.2.2: The buck DC/DC converter.

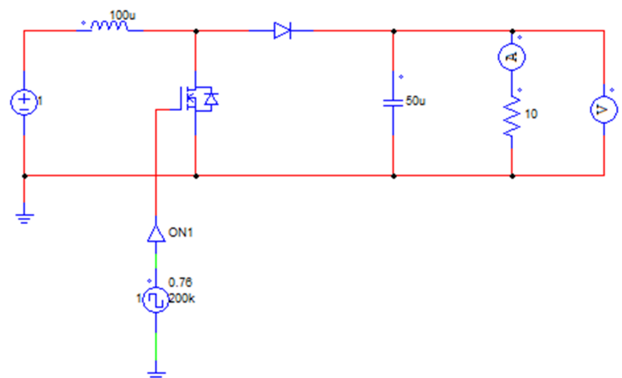

Figure 3.2.3: The boost DC/DC converter.

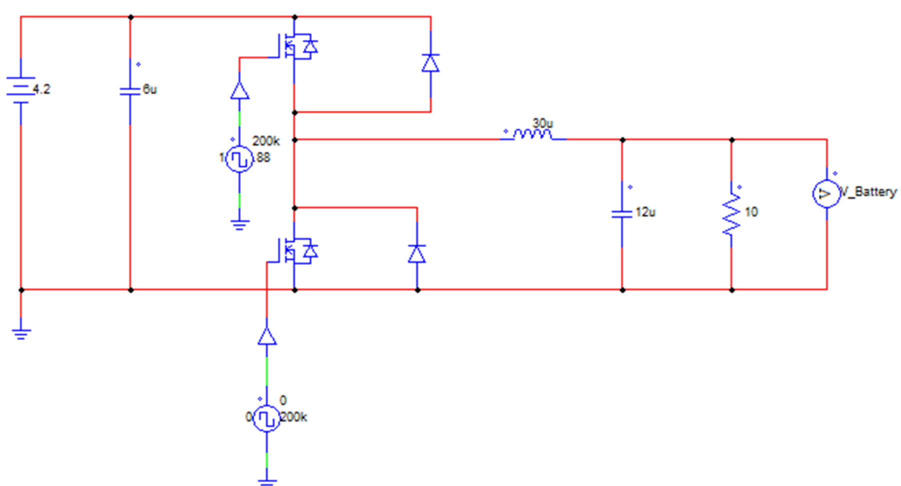

Figure 3.2.4: The bidirectional buck-boost DC/DC converter.

After ensuring that each converter was outputting accurate values, they were then interconnected with each other by referencing the overall schematic design given in figure 2.3.4. This overall design was designed using PSIM software and is given in figure 3.2.5. In this topology, the buck and boost converters are providing the power necessary for WSN operation and battery charging. The buck is bucking the solar panel to a desired voltage value of 4.2v with an accuracy rating within 1% error. The boost converter is performing its task of delivering power from the brushless wind turbine to the output test resistor (approximately 4.2 v). These voltages are then regulated by the bidirectional buck-boost converter to charge the lithium-ion battery. In this design, the lithium-ion battery is left out as the power stage was the focus. The two switches on the bidirectional will control the charging and discharging scheme. Depending on the voltage supplied, which in this case is 4.2 v, then it will charge or discharge. Should the voltage be less, then both the switches of the mosfets on the buck and boost converters will be turned off by the microcontroller, and the discharging switch for the bidirectional buck-boost converter will be turned on - allowing for power when the two ambient sources were not providing enough power for the system.

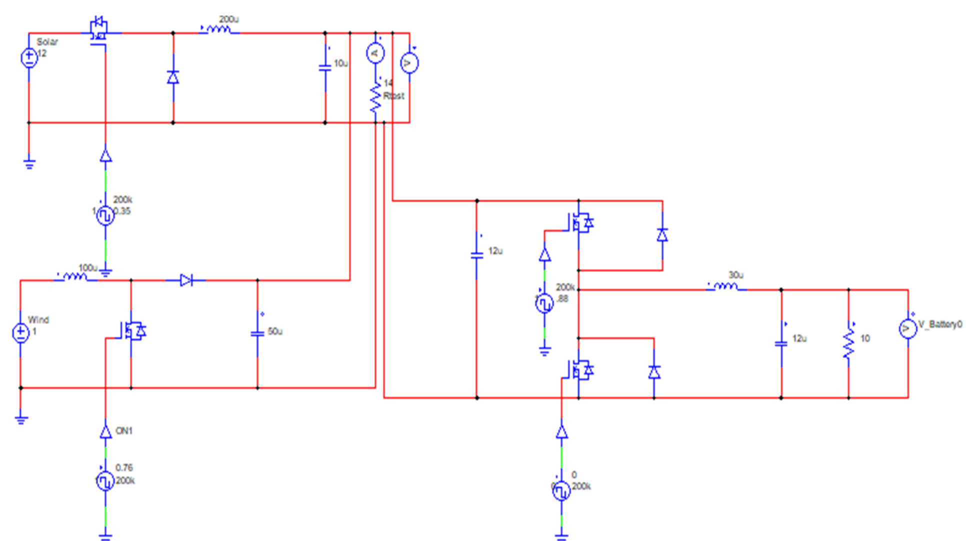

Figure 3.2.5: PSIM schematic of converters connected.

Due to recent events, the project had to shift from PSIM to simulink. The PSIM converters were then converted to simulink models. The following figures are the converted buck, boost, and bidirectional buck-boost converters. Figure 3.2.6 shows the buck converter with feed-back control. Feedback control was accomplished by taking the output voltage and referencing it with a 4.2 voltage signal. This was then scaled and compared to be outputted to the gate signal of the mosfet switch. The control allowed for less voltage ripple and achieved our objective of having less than 1% error. Figure 3.2.7 shows the results of this converter. The output ranges from between 4.241 and 4.241v. There was almost no voltage ripple from this converter. This simulation result shows that the buck converter is operating within the specified range and that design of the converter was successfully implemented.

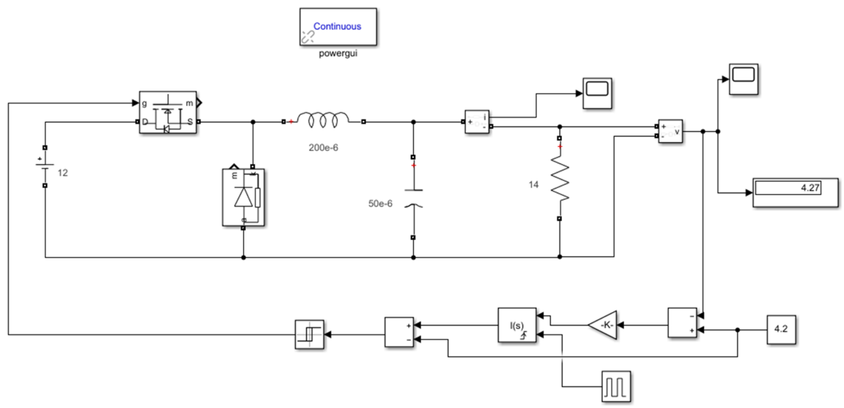

Figure 3.2.6: Simulink schematic of buck converter with feedback design.

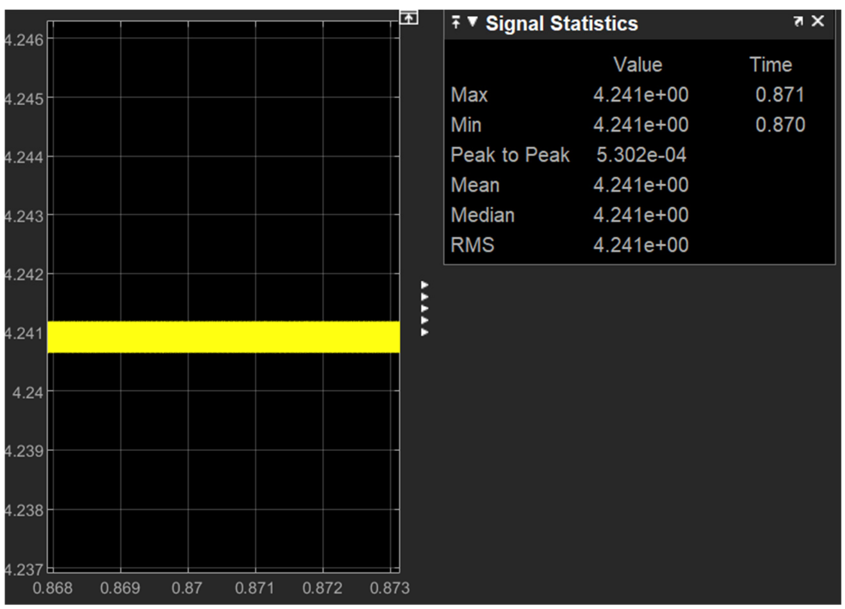

Figure 3.2.7: Simulink results of buck converter with feedback design.

Figure 3.2.8 shows the boost converter with feed-back control. Feedback control was accomplished by taking the output voltage and referencing it with a 4.2 voltage signal. This was then scaled and compared to be outputted to the gate signal of the mosfet switch. The control allowed for less voltage ripple and achieved our objective of having less than 1% error. Figure 3.2.8 shows the results of this converter. The output ranges from between 4.296 and 4.29 v. There is almost no voltage ripple from this converter. This simulation result shows that the boost converter is operating within the specified range and that design of the converter was successfully implemented.

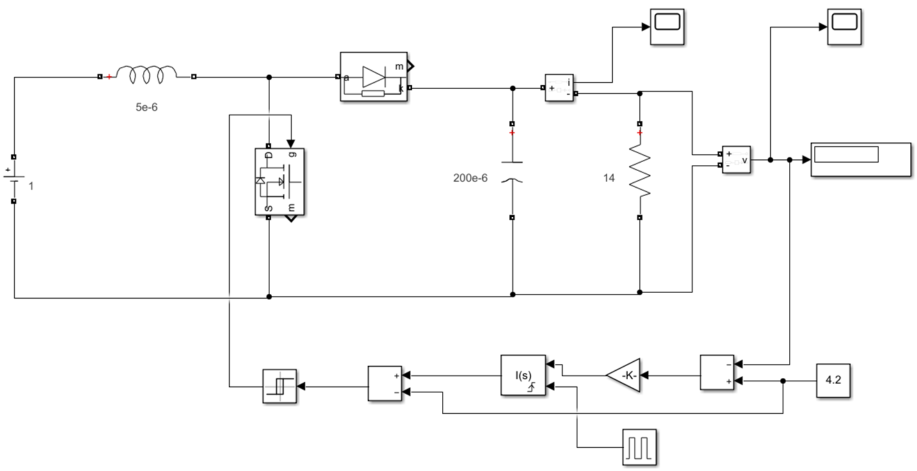

Figure 3.2.8: Simulink schematic of boost converter with feedback design.

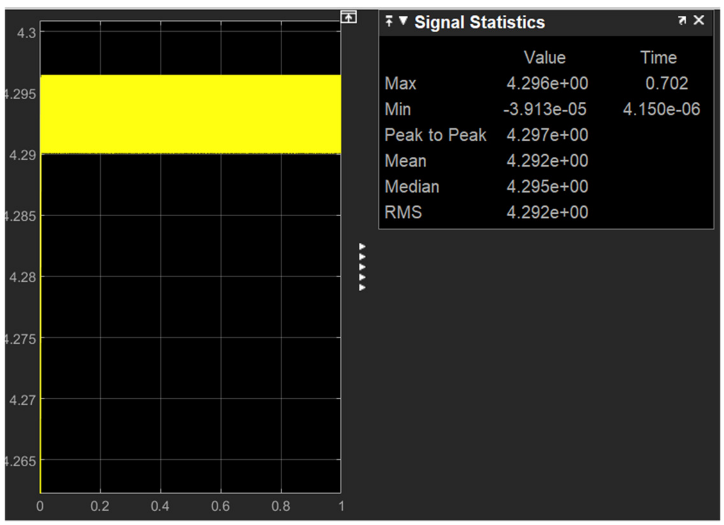

Figure 3.2.9: Simulink results of boost converter with feedback design.

In figure 3.2.10, the simulink schematic for the bidirectional buck-boost converter is shown. The two switches are used to operate the converter in charge and discharge mode. In charging mode, the converter will receive 4.2 v from the buck and boost converters from the solar and wind harvesters. It will then buck this voltage down to the necessary charging voltage for the lithium ion battery. The battery will charge as a result. When there is no voltage input, meaning the two energy harvesters are not providing enough power, the battery will discharge via the bidirectional buck-boost converter. It will boost the nominal voltage output from the battery. This voltage is approximately 3.7 v. It will boost this voltage to the required voltage level. Since these voltages are relatively stable, there is no need for feedback control for the charge or discharge mode. Figure 3.2.11 shows the results of this converter when charge mode is enabled. The scope captures the state of charge of the battery, the current, and the voltage. In this figure, the battery is being charged. SOC is linearly increasing as it should. In figure 3.2.12, the battery is discharged. SOC is linearly decreasing as shown in the figure. These simulation results show that the bidirectional buck-boost converter was implemented correctly.

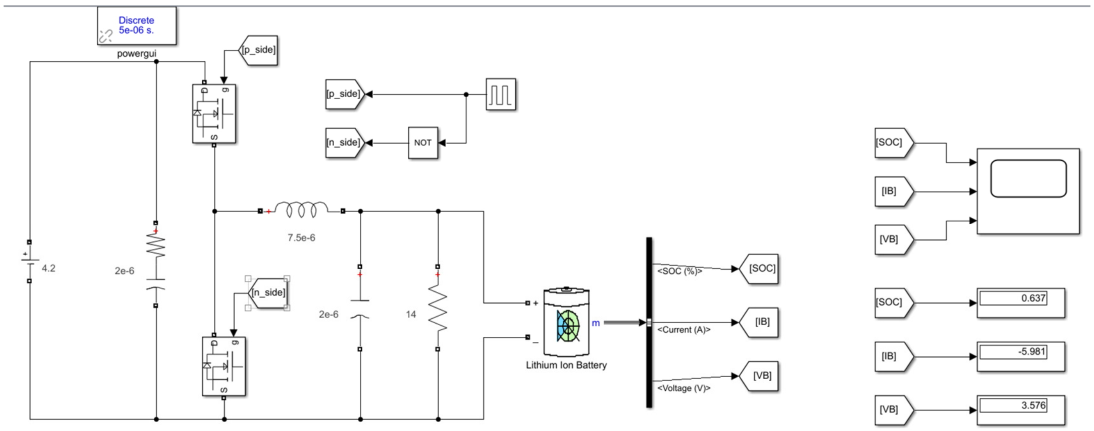

Figure 3.2.10: Simulink schematic of bidirectional buck-boost converter.

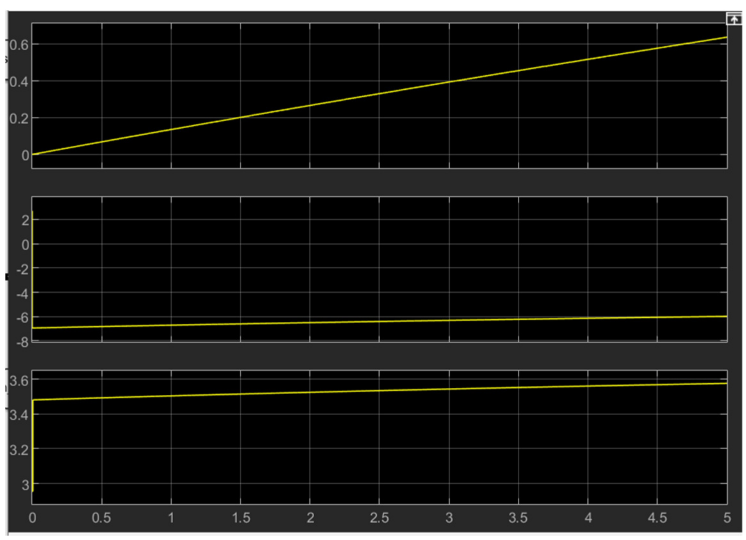

Figure 3.2.11: Simulink result of charging bidirectional buck-boost converter.

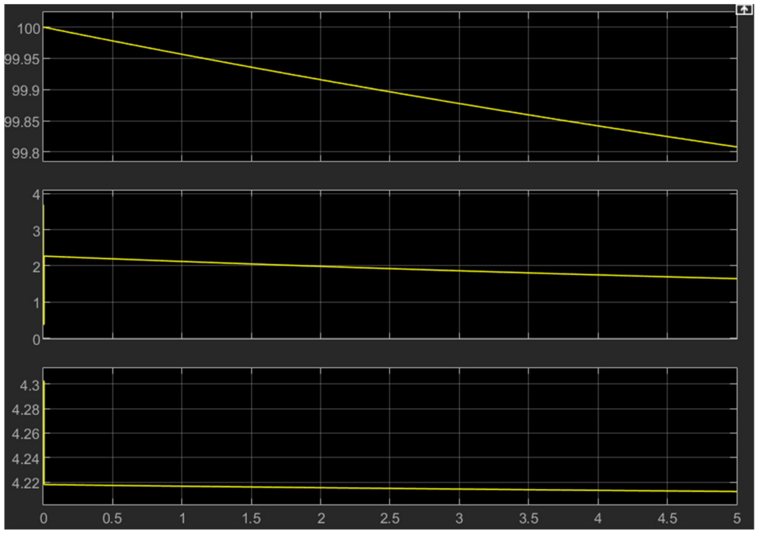

Figure 3.2.12: Simulink result of discharging bidirectional buck-boost converter.

After ensuring that each converter was outputting accurate values, they were then interconnected with each other by referencing the overall schematic design given in figure 2.3.4. The overall design was designed using simulink and is given in figure 3.2.13. In this topology, the buck and boost converters are providing the power necessary for WSN operation and battery charging. The buck is bucking the solar panel to a desired voltage value of 4.2v with an accuracy rating within 1% error. This result was obtained from simulating the buck in simulink. The boost converter is also performing its task of delivering power from the brushless wind turbine to the output test resistor. The simulink simulation for this converter outputted the desired value. These voltages are then regulated by the bidirectional buck-boost converter to charge the lithium-ion battery. In this design, the lithium-ion battery was used. The two switches on the bidirectional will control the charging and discharging scheme. Depending on the voltage supplied, which in this case should be 4.2 v, then it will charge or discharge. Should the voltage be less than this value, then both the switches of the mosfets on the buck and boost converters will be turned off by the microcontroller, and the discharging switch for the bidirectional buck-boost converter will be turned on - allowing for power when the two ambient sources were not providing enough power for the system. Discharging will decrease the state of charge of the battery which will be monitored by the microcontroller by coulomb counting.Voltage and current control will also be done using the microcontroller to ensure that the battery does not draw too much power from the two converters.

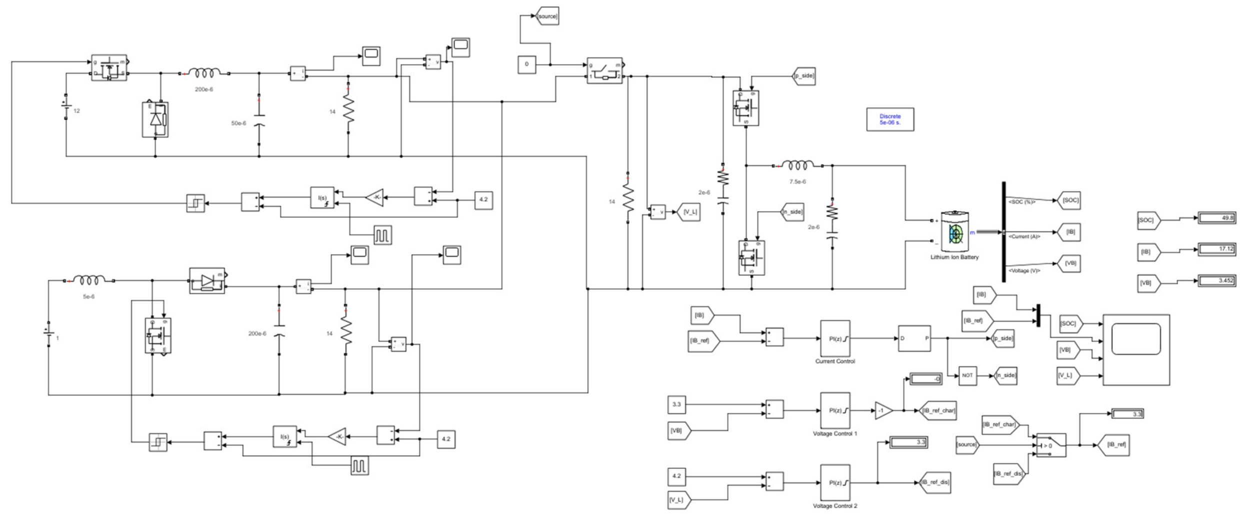

Figure 3.2.13: Simulink schematic of overall design.

3.3 Conclusion

The primary objective of this project was to design and implement a compact and self-sufficient, source-harvesting power system for WSN. As such, our tasks were to design and implement converters and then control the power stage through the use of microcontrollers. The power stage of this project was designed using three converters: buck, boost, and bidirectional buck-boost. The buck converter was used for solar harvesting. Wind harvesting was done using the brushless wind turbine and the boost converter. The bidirectional buck-boost converter served the purpose of distributing power from and to the battery. These converters were dynamically managed by the STM32 microcontroller. The MPPT algorithm was implemented to ensure that maximum power from both the wind and solar harvester were maximized and efficiently used. Incremental conductance was used for this purpose. Current and voltage sensors were necessary for this task. These operations allowed for the microcontroller to efficiently manage the converters and lithium ion battery. By dividing the tasks between ourselves, we were able to design and simulate the power management system for hybrid source harvesting. Physical implementation was not possible due to recent events. Future work of this project would include a physical model with a micro-managed, hybrid power system. If necessary, additional power sources and harvesting devices could be added to assure longevity of the lithium ion battery. Overall, this project provided hands-on design and implementation of power systems and helped further reinforce our understanding on fundamental engineering. Even though a physical prototype was not implemented, the trials and errors that came about during the experimental and simulation phases helped deepen our previous understandings of our respective engineering fields. As such, this project was able to provide us necessary experience to improve our knowledge and expertise in our respective fields. This experience will continue to help us to further carve out our career paths in the future.

4. IEEE Standards

IEEE Standard 802.15.4

- General Standard for LR-WPAN
- Data Rate Standard
- Transmission Range Standard
- No network layer defined
- Full Function Device vs. Reduced Function Device
- Operate within the specified frequency band
- Ultra low complexity, cost, power consumption, and data rate wireless communication for inexpensive devices

Table 5.2: New proposed schedule.

GANTT CHART

PROJECT TITLE	Energy Harvesting for WSN
PROJECT MEMBERS	Lawrence Brieno, Lee Lor, Alwin Villamor

WBS NUMBER	TASK TITLE	TASK MEMBER	START DATE	DUE DATE	DURATION	PCT OF TASK COMPLETE
1	**Design**					
1.1	Boost converter Parameters	Lee, Lawrence	12/4/19	12/31/19	27	45%
1.2	Simulate Boost Parameters	Lee, Lawrence	12/6/19	1/14/20	38	10%
1.3	MPPT Algorithm	Alwin	10/23/19	1/14/20	81	10%
1.4	Feedback Controller	Lawrence	12/21/19	1/14/20	23	5%
1.5	Voltage Mode Matlab Design	Lee, Lawrence	12/21/19	1/14/20	23	5%
1.6	Battery Charging Scheme	All Memebrs	1/1/20	1/21/20	20	10%
2	**Testing**					
2.1	Buck-Boost Simulation	Lee, Lawrence	12/26/19	1/21/20	25	22%
2.2	MPPT Algorithm	Alwin	10/24/19	12/26/19	62	16%
2.3	Feedback Controller with Buck Boost	Lawrence	1/10/20	2/1/20	21	0%
2.4	Tune Feedback and Buck-Boost	Lee, Lawrence	1/10/20	2/1/20	21	0%
2.5	Solar and Wind Implementation	All Memebers	1/21/20	2/21/20	30	0%
3	**Hardware**					
3.1	Ordering components	All Members	1/21/20	1/31/20	10	0%
3.2	Hardware measruremnt and calculation	All Members	1/30/20	2/14/20	14	0%
3.3	microcontroller	Alwin	1/1/20	2/7/20	36	10%
3.4	PCB design	All Members	2/15/20	3/1/20	16	0%
3.5	Housing desing	All Members	1/1/20	2/14/20	43	0%
4	**Reports/Presentations**					
4.1	Draft Proposal	All Members	9/5/19	10/23/19	48	100%
4.2	Final Oral Presentation	All Members	11/1/19	12/11/19	40	90%
4.3	Final Proposal	All Members	10/23/19	12/18/19	55	85%
4.4	Oral Progress Report	All Members	10/14/19	10/23/19	9	100%

6. References

[1] "How Do Wind Turbines Work?" Energy.gov.
Available: https://www.energy.gov/eere/wind/how-do-wind-turbines-work.

[2] "Digital control strategy for a buck converter operating as a battery charger for stand-alone photovoltaic systems" Science Direct. Available: https:/ www. sciencedirect.com/science/article/pii/S0038092X16305217

[3] Richard G. Belu, Richard Chou, Lucea Ionel Cioca. "Design a Micro-wind and Solar Energy Harvesting System for a Wireless Sensor Node to Operate in Coastal and Marine Area as a Senior Design Project" Semanticscholar.org. Available:https://pdfs .semanticscholar.org/c56a/43902719aff5409603b6a7a889e890a3d152.pdf

[4] Balamurugan, T. and Manoharan, S. "Optimal Power Flow Management Control for Grid Connected Photovoltaic/Wind turbine/Diesel generator (GCPWD) Hybrid System with Batteries." Researchgate.net. Available:https://www.researchgate.net/publication /_ Control _for_Grid_Connected_PhotovoltaicWind_turbineDiesel _generator_ GCPWD _Hybrid_System_with_Batteries#pf4 [Accessed 16 Oct. 2019].

[5] Ayman Fayed, Bora Tar. "An Overview of the Fundamentals of Battery Chargers," *2016 IEEE 59th International Midwest Symposium on Circuits and Systems,* 16-19 October 2016.

[6] M. A. Abdullah, A. H. M. Yatim and Chee Wei Tan, "A study of maximum power point tracking algorithms for wind energy system," *2011 IEEE Conference on Clean Energy and Technology (CET)*, Kuala Lumpur, 2011, pp. 321-326.

[7] T. Salma, R. Yokeeswaran, "Incremental Conductance Technique for a Hybrid Wind - Solar Energy System," 2014 *International Journal of Science and Research (IJSR), Volume 3 Issue 5,* pp. 612-615 (2014)

[8] Tektron Genesis, *Advantages and Disadvantages of Surface Mount Technology,* March 8, 2018. [Online]. Available:https://medium.com/@tektrong/advantages-disadvantages-of- surface-mount-technology-smt-100e0f16a17

[9] "Microcontroller based bidirectional buck–boost converter for photo-voltaic power plant" Science Direct. Available:
https://www.sciencedirect.com/science/article/pii/S231471721730017X

Appendix A

The following code shows the voltage mode controller crossover frequency parameters, which was used to design and demo the circuit in Figure 3.1.

```
%% ECE 186A

%% Transfer Function, Buck Converter

%Initializing values
r = 0.2;
C = 820*10^-6;
L = 160*10^-6;
Vin = 42;
R = 0.2;

% defining "s" for the transfer function
s = tf('s');

G = (Vin/(L*C))*((1+s*r*C)/((s^2) + s*((1/(R*C)) + (r/L))+(1/(L*C))));


% The small signal output voltage and duty ratio will be named "G"


options = bodeoptions;

options.FreqUnits = 'Hz'; %converting rad/s to Hz.

bode(G,options)
grid on
```